Tube Dynamics in Binary Polymer Blends

Jung Hun Lee, Lewis J. Fetters, and Lynden A. Archer*

School of Chemical and Biomolecular Engineering, Cornell University, Ithaca, New York 14853

Adel F. Halasa

Chemical Division R&D, Goodyear Tire and Rubber Company, Akron, Ohio 44305

Received April 29, 2004; Revised Manuscript Received July 21, 2004

ABSTRACT: Stress relaxation dynamics of entangled linear/linear and short star/linear 1,4-polybutadiene and 1,4-polyisoprene blends are studied using a combination of mechanical rheometry and theory. In binary blends comprised of long linear chains and entangled short star or short linear molecules, we find that relaxation of the faster relaxing "short" molecules leads to a reduction in shear modulus consistent with expectations for solventlike dilution of the entanglement network in which the slower relaxing "long" chains diffuse. Terminal relaxation dynamics of the long chains are nonetheless found to be substantially different in blends with short star and short linear molecules. Specifically, while terminal relaxation in linear/linear blends is consistent with expectations for reptation diffusion of the long linear molecules in a uniformly dilated tube, terminal relaxation in the short star/linear blends occur by reptation diffusion of the long chains in an undilated tube. Thus, in the short star/linear blends the longer linear chains appear unable to take advantage of the more dilated network produced by relaxed stars, even when relaxation times of the two species differ by more than 2 orders of magnitude. This finding is inconsistent with expectations from dynamic tube dilation models for polymer blend relaxation. It indicates that architecturally complex molecules exert a longer-lived influence on tube equilibration in blends than anticipated by these models.

Introduction

Stress relaxation dynamics of narrow molecular weight distribution entangled linear and simple starlike branched polymers are well described by the reptation/tube model, when analytical formulas for contour length fluctuations (CLF),[1] and dynamic dilution (DD),[2] proposed by Milner and McLeish are added to the original tube model framework of de Gennes and Doi–Edwards.[3,4] CLF describes thermal motion of chain ends as they explore portions of the tube without movement of the entire chain,[4] and DD assumes that relaxed portions of a polymer chain act as an effective solvent for the unrelaxed portions.[2,5] The tube model including the CLF and DD formulas proposed by Milner and McLeish, here termed the MM-model, has also been reported to yield reasonable predictions for the dynamic shear moduli ($G'(\omega)$ and $G''(\omega)$) of entangled star/linear polymer blends in which the star is the slower relaxing component.[6,7] Addition of a constraint-release Rouse relaxation mechanism (CR) to the MM-model framework, wherein the tube confining unrelaxed star arm segments explores (by Rouse motion) the dilated network ("super-tube") created by relaxed linear chains, improves agreement between theoretical predictions and experimental observations for star/liner blend dynamics on intermediate and long time scales.[6]

The first analytical equations for tube Rouse dynamics in star/linear polymer blends,[6] can be readily traced to CR theories for binary blends of linear polymers proposed by Doi et al.[8] and Viovy et al.[9] In these theories the idea of tube equilibration by Rouse motion of a primary confining tube in a secondary, dilated super-tube was first developed. An unusual assumption made in extending these CR theories to star/linear blends is that relaxation of unrelaxed star arm segments is frozen while the tube equilibration process proceeds.[6] While

this assumption appears to be valid for blends of well entangled stars and linear chains,[6,7] presumably because the branch point of the slower relaxing stars suppresses relaxation of the unrelaxed arm segments, it has heretofore not been evaluated in linear/linear blends and blends of faster relaxing star molecules and slower relaxing "long" linear chains. Indeed the full CR tube relaxation process found for star/linear blends,[6,7] is in principle applicable to intermediate and long-time dynamics in other polymer blend systems (e.g., linear/linear, short-star/linear, asymmetric star/linear and multiarm (pompom)/linear), but is also untested in any of these materials.

Blends of entangled long linear chains and short, but entangled, star or linear polymer molecules provide perhaps the simplest model systems for further evaluating the MM-model with tube Rouse CR dynamics. For a star polymer with fixed arm molecular weight, dynamics in the materials studied in refs 6 and 7 can be made more complex by gradually increasing the length of the linear chain. Beyond a certain linear chain molecular weight, sections of the linear molecules will remain unrelaxed after relaxation of the star arms. While it is possible that these linear chain sections might eventually relax by the same CR tube equilibration process observed in blends of slower relaxing stars in linear hosts, it is unclear apriori whether this process can ever be competitive with reptation diffusion of unrelaxed linear chain segments in their original (undilated) tube.

In bidisperse blends comprised of entangled short (molecular weight M_s) and long (molecular weight M_l and volume fraction ϕ_l) linear chains, the final entanglement density $z_t = M_l \phi_l{}^\alpha / M_e$ of the more slowly relaxing long chains and the relative rates of long chain reptation $\tau_d = 3\tau_e [M_l/M_e]^3$ and CR Rouse relaxation, $\tau_{d*} = 3\tau_e [M_s/M_e]^3 [M_l/M_e]^2$, determine the terminal blend dynamics.[8–10]

Here α is the dilution exponent and complexities due to CLF are ignored in the definitions for both time scales. Provided the long and short polymer chains are chemically identical and well entangled, $\alpha = 4/3$.[7,11] However $\alpha = 1$ is a common choice for scaling theories.[2,6,8−10] The parameter $G_r \equiv 3\tau_e(M_l/M_e)^3/3\tau_e(M_s/M_e)^3(M_l/M_e)^2 = M_e^2M_l/M_s^3$ therefore provides a convenient way to express this ratio of time scales. In cases where the long chains remain entangled even after short chain constraints are lost, i.e., $z_t > 1$, and $G_r < 1$ theory suggests that reptation diffusion of the long linear chains in their original undilated tubes should be more competitive with CR tube dynamics for relieving stress at long times.[8,9]

Recently, Park and Larson[12] incorporated tube Rouse CR motion into the MM-model framework to predict stress relaxation of several blends of short (M_s) and long (M_l) linear chains. These authors reported that for $G_r > G_{rc} \approx 0.064$, the long chain reptates in a tube dilated by the faster relaxing shorter chains. This value of G_{rc} is substantially lower than the estimate of unity based on a naive comparison of τ_d and τ_{d*}, which means that terminal relaxation by reptation of long linear chains in an undilated tube is much less competitive than anticipated from the scaling analyses of Doi et al.[8] and Viovy et al.[9] It is nonetheless important to point out that other studies have found values of G_{rc} closer to unity in linear/linear blends with $z_t > 1$,[10,13] indicating that this parameter alone is probably insufficient to unambiguously characterize terminal dynamics in bidisperse linear polymer blends.

More recently, Watanabe et al.[13] measured the dielectric relaxation $\Phi(t)$ and stress relaxation $\mu(t)$ functions for bidisperse linear blends of cis-polyisoprene. The authors compared the stress relaxation function expected for complete dilation of the tube in which the long chains relax $\mu_{DTD}(t) = [\Phi(t)]^{1+\alpha}$ with the measured $\mu(t)$ to study the effect of dynamic tube dilation (DTD) on stress relaxation of bidisperse blends; α, the dilution exponent, is taken to be 1.3. For blends with long chain volume fractions above 0.05, good agreement between $\mu(t)$ and $\mu_{DTD}(t)$ was observed at both short and long times, but not at intermediate times. On the basis of these observations, Watanabe et al. conclude that terminal dynamics of the longer chain in the blends can occur in a dilated tube only on time scales longer than a certain concentration-dependent time required for CR equilibration of entanglement segments of the longer chains in the dilated tube. Implying that the motion of long chains in bidisperse blends become free from the entanglement effect of short chains only after the CR equilibration time.

In this article, we discuss stress relaxation of bidisperse linear/liner and short star/linear blends to further investigate tube dilation/CR equilibration dynamics in polymer mixtures. The arm length of the star is chosen so that the terminal relaxation time of the pure stars is comparable to that of the short linear polymers. Two simplified microscopic situations are considered in detail for evaluating dynamics of the slower relaxing linear chains: (i) reptation in a dilated tube with the CR tube motion[6] and (ii) reptation in an undilated tube without the CR tube motion. Polymer molecular weights and blend concentrations are selected to study the three primary modes by which the orientation of slower relaxing, longer molecules can equilibrate:

(1) If the terminal relaxation time of the lower molecular weight blend component is comparable to that of the higher molecular weight (long) linear molecules, reptation of the long chains is fast compared to constraint release and tube dilation. In this case the long linear polymer is anticipated to relax primarily by reptation diffusion in an undilated tube without CR motion (UDT mode).

(2) If the relaxation time of the two polymers are well separated, but the long linear polymer reptation rate is fast in comparison to tube equilibration, the perforated (by CR) network surrounding the more slowly relaxing long chains has no effect on terminal relaxation. In this case, CR motion only changes the dynamic modulus of the blend on intermediate time scales, but terminal relaxation of the long chains occurs by reptation in the original (undilated) tube (UDT wCR mode).

(3) If constraint release and tube equilibration are fast in comparison to reptation, terminal relaxation in the blend proceeds by reptation of the long chains in a dilated tube (TD mode).

To provide a comprehensive understanding of the strengths/limitations of these scenarios, we will use the MM-model framework as a tool for evaluating stress relaxation in polymer systems under each of the above situations. The quality of the model predictions for the dynamic modulus of the blends is evaluated by direct comparison to the experimentally measured moduli and used to establish the accuracy/relevance of the underlying molecular-scale physics in the model. We believe this approach is advantageous because it introduces no new effects that can, for example, occur when experimental methods are used to decouple the various modes of terminal relaxation. The approach nonetheless assumes that the basic MM-model framework[1,2,6] is correct, which could be problematic in case 1 when all three effects operate simultaneously.

Experimental Section

Narrow distribution linear 1,4-polybutadiene (PBD) polymers used in the study were purchased from Polymer Source, Inc. The 1,4-polybutadiene 4-arm-star (GYS) was obtained from Goodyear R&D Division. The 1,4-polyisoprene (PI) linear and 3-arm star (S) polymers used in the study were synthesized in-house using anionic techniques under high vacuum conditions. All polymers were extensively characterized (see Table 1) by size exclusion chromatography (SEC) with a laser light scattering detector (TDA 302 with 4 mixed-bed columns, Viscotek). The microstructures of the polymers were characterized using ^{1}H NMR analysis[14] and the results are also provided in Table 1.

The PI polymerization was carried out using degassed cyclohexane and isoprene monomer, which were purified by *n*-butyllithium prior to distillation to the reaction vessel. The living linear chains was initiated by *sec*-butyllithium in cyclohexane at ambient temperature inside a M-Braun Labmaster glovebox (MBraun, Inc.) and terminated by the addition of degassed methanol. For PI star polymers, methyl trichlorosilane (CH_3SiCl_3), which acts as a branch point, was purified by distillation into an ampule after degassing. To obtain a 3-arm star polymer, CH_3SiCl_3 linker was allowed to react with a small excess of the living linear chains, which become star arms. During the branching reaction, changes in molecular weights were monitored to verify the desired structure is obtained (see Figure 1). While the peak at higher elution volume indicates the initial living arm, the peak at lower elution volume indicate the desired 3-arm star polymer. It is evident from the figure that the initial living arm is transformed to the 3-arm star polymer via a two-arm star intermediate, indicating that branches add sequentially to the

Table 1. Molecular Characterization

sample	M_n (SEC with LS) [g/mol]	PDI[d]	M in model [g/mol]	% microstructure by ^{1}H NMR (1)1,4; (2)1,2; (3)3,4
		1,4-Polybutadiene		
L25K	25 800	1.01	25 800	(1) 92.0 (2) 8.0
L74K	74 100	1.01	74 100	(1) 91.4 (2) 8.6
L161K	161 600	1.01	161 600	(1) 92.0 (2) 8.0
L395K	395 000	1.02	395 000	(1) 92.2 (2) 7.8
GYS	36 300[a] 10 000[b,c]	1.07	11 500[b]	(1) 92.0[c] (2) 8.0[c]
		1,4-Polyisoprene		
N250K	256 900	1.01	280 000	(1) 94.2 (3) 5.8
S	96 400[a] 33 000[b]	1.02 1.01	32 000[b]	(1) 92.9 (3) 7.1

[a] Total molecular weight (M_{total}). [b] Arm molecular weight (M_{arm}). [c] Values from Chemical Division R&D of Goodyear company. [d] PDI: polydispersity index.
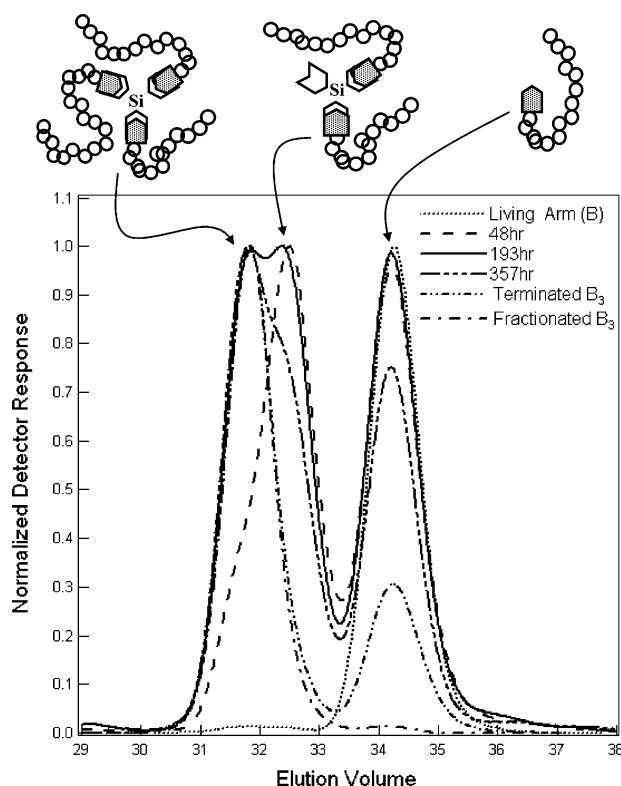
Figure 1. GPC analysis of samples taken during the branching reaction of polyisoprene 3-arm star polymer (S).

chlorosilane linking agent. The desired 3-arm star polymers were separated from unreacted arms in the terminated crude product by repeating toluene/methanol fractionation. Molecular weights and polydispersity indices of all polymers used in the study are summarized in Table 1.

Short linear PBD and GYS were blended with long linear PBD at different weight fractions in excess cyclohexane. Other linear/linear PBD blends and PI star (S) blends with long, linear PI (N250K) were prepared in the same manner. Following complete dissolution of the polymers, cyclohexane was driven off in a vacuum oven at room temperature. For brevity, sample names are coded by molecular weight of the long linear chain and fraction of the faster relaxing linear or star molecules in the blends. For example, GL161K50 refers to GYS

and L161K blend with 50 wt % of GYS ($\phi_{GYS} = 0.5$) and L25L395K40 refers to L25K and L395K blend with 40 wt % of L25K ($\phi_{L25K} = 0.4$).

Rheological measurements were performed using a Rheometrics ARES-LS rheometer in an oscillatory shear mode with 10 mm or 12 mm diameter parallel-plate geometry. Terminal/low-frequency dynamics of all blend samples were obtained at 28 °C. To obtain the intermediate frequency relaxation responses, the low frequency data were supplemented by low temperature experiments. The RSI Orchestrator software was used to automatically derive master curves at a reference temperature 28 °C by a two-dimensional residual minimization technique.

Results and Discussion

Dynamic storage, $G'(\omega)$, and loss, $G''(\omega)$ of the short star (GYS) and short linear (L25K) PBD melts are shown in Figure 2a. But for the more pronounced maximum in $G''(\omega)$ of the linear molecule, just prior to the onset of the terminal regime, the relaxation behavior of the two polymers is qualitatively similar. The location of the $G'(\omega)-G''(\omega)$ crossover point is also similar for the two polymers, indicating that their average terminal relaxation times are close. Figure 2b are the storage and loss moduli for 50/50 blends of L25K and GYS with a much higher molecular weight linear polybutadiene (L161K). The ratio of the weight-average relaxation time of the pure L161K melt to that of the pure faster relaxing blend component can be estimated from the reciprocal of the frequency at which the imaginary part (η'') of the respective complex viscosities manifest local maxima in the terminal zone, $\bar{\tau} = 1/\omega_{\eta''}$, and $\bar{\tau}_{L161K}/\bar{\tau}_{L25K} \sim 618$ and $\bar{\tau}_{L161K}/\bar{\tau}_{GYS} \sim 212$. Despite the similarities of the short star and linear polymer dynamics in the melt, Figure 2b shows that these two molecules have quite different qualitative influences on the overall blend relaxation dynamics. For example, while two distinctive $G''(\omega)$ maxima and minima appear in L25L161K50, consistent with expectations for a symmetric linear/linear blend comprised of components with well-separated relaxation times, $G'(\omega)$ and $G''(\omega)$ for GL161-K50 decrease nearly monotonically from the rubbery plateau to the terminal regime, with a barely recognizable kink/inflection just before the $G'(\omega)-G''(\omega)$ crossover point.

A second minimum in $G''(\omega)$ is also evident in L25L161K50 at low frequency, indicative of a second rubbery plateau. Comparing the storage modulus G_I at the first loss minimum to the storage modulus G_{II} at the second minimum we find $G_{II}/G_I \approx \phi_l^{2.5(\pm 0.3)}$, which is the result expected if the entanglement network in which high molecular weight linear chains (l) relax, is diluted with a nonpolymeric Θ solvent. In the case of L25L161K50 G_I is close to the melt plateau modulus for entangled PBD, indicating that the network dilution effect observed at low frequencies is a dynamic phenomenon. That is, the enlarged entanglement spacing due to the relaxation of faster relaxing chains appears as a second rubbery plateau G_{II} only at low frequencies. In the case of the star/linear blend (GL161K50), only a hint of the second, low-frequency, loss minimum is evident. The ratio of the storage modulus corresponding to this minimum to that at the high-frequency loss minimum is also consistent with expectations for the network dilution effect. However, the much weaker loss minimum observed for GL161K50 implies that despite this effect, terminal relaxation dynamics do not proceed by simple reptation diffusion of the slower relaxing linear chains in an enlarged tube.
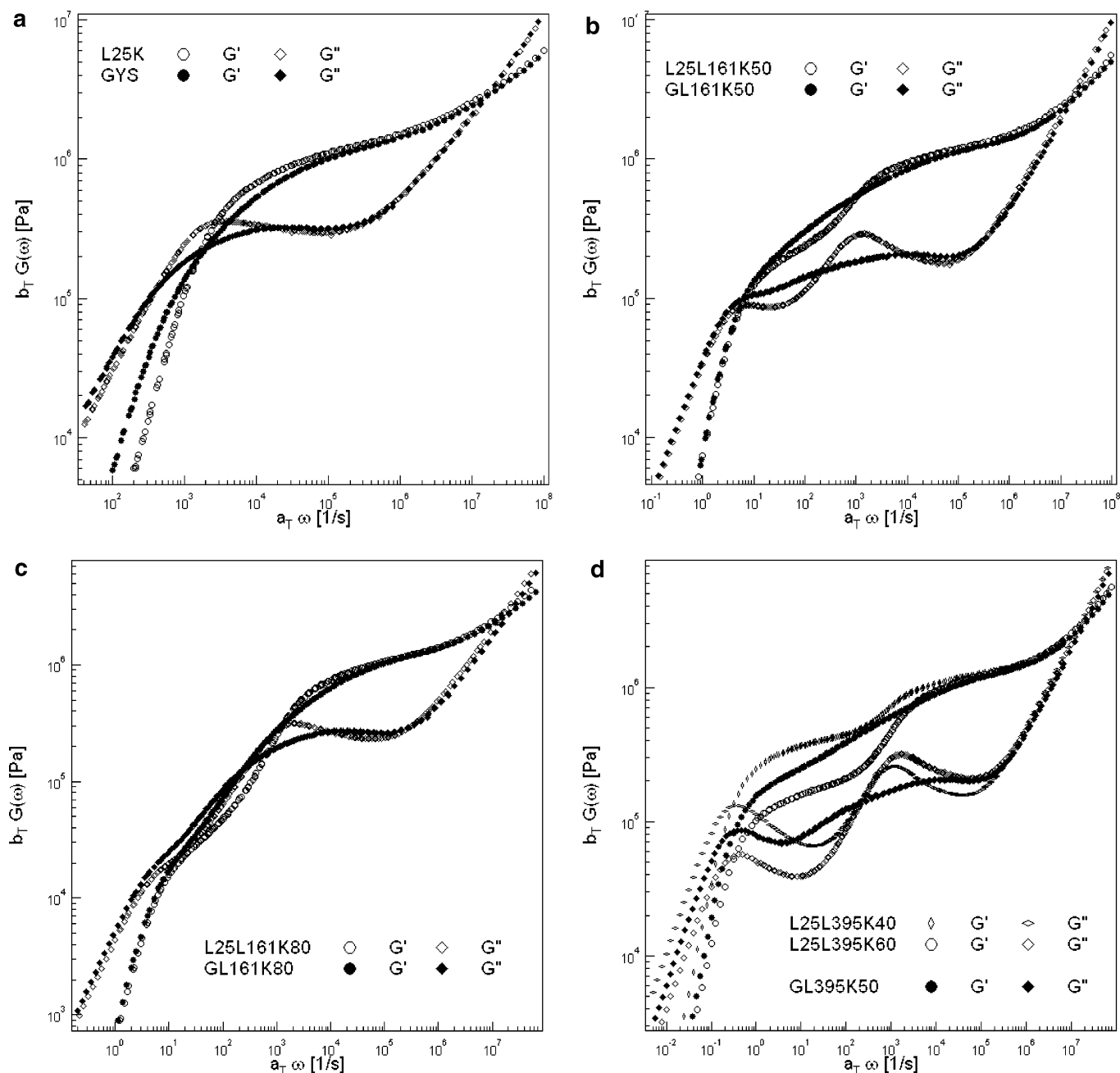
Figure 2. Dynamic moduli, $G'(\omega)$ and $G''(\omega)$, (a) for polybutadiene short linear (L25K) and short arm star (GYS) polymers, (b) for short linear/linear blend (L25L161K50) and short arm star/linear blend (GL161K50), where the fraction of long linear polybutadiene (L161K) is $\phi_l = 0.5$, (c) for short linear/linear blend (L25L161K80) and short arm star/linear blend (GL161K80), where the fraction of long linear polybutadiene (L161K) is $\phi_l = 0.2$, and (d) for short linear/linear blends (L25L395K40 and L25L395K60) and short arm star/linear blend (GL395K50), where the fractions of long linear polybutadiene polymers (L395K) are $\phi_l = 0.6$, 0.4 and 0.5, respectively. The reference temperature is 28 °C.

Figure 2c shows the measured $G'(\omega)$ and $G''(\omega)$ for the same polymers in 2b, except with a lower volume fraction of the higher molecular weight linear polymer ($\phi_{L161K} = 0.2$). In this case the second loss minimum is not apparent for either of the blends, and power-law Rouse-like terminal behavior is evident for both materials. Again, $G'(\omega)$ and $G''(\omega)$ for the two materials almost overlap at very low frequencies. At intermediate frequencies $G'(\omega)$ and $G''(\omega)$ are generally higher for the star/linear blend (GL161K80), even though their plateau modulus is marginally lower. These observations suggest that the contribution of star arms to stress relaxation of longer linear chains is longer-lived than that of the short linear chains, even if the stars and short

linear molecules possess comparable relaxation times in the melt.

It is evident from the GL-series star/linear blend results that any tube dilation arising from relaxed short star chains can be better isolated in binary blends containing even higher molecular weight linear chains. Figure 2d summarizes experimental $G'(\omega)$ and $G''(\omega)$ data for blends of short linear and short star PBD molecules with a much longer linear PBD (L395K). In this case, the ratio of the weight-averaged relaxation time of the pure linear and star melts, $\bar{\tau}_{L395K}/\bar{\tau}_{GYS}$, is 3600 and $G_r = 0.075$ for the linear/linear blend. On the basis of the work of Park and Larson,[12] we would therefore expect terminal dynamics in the L25L395K
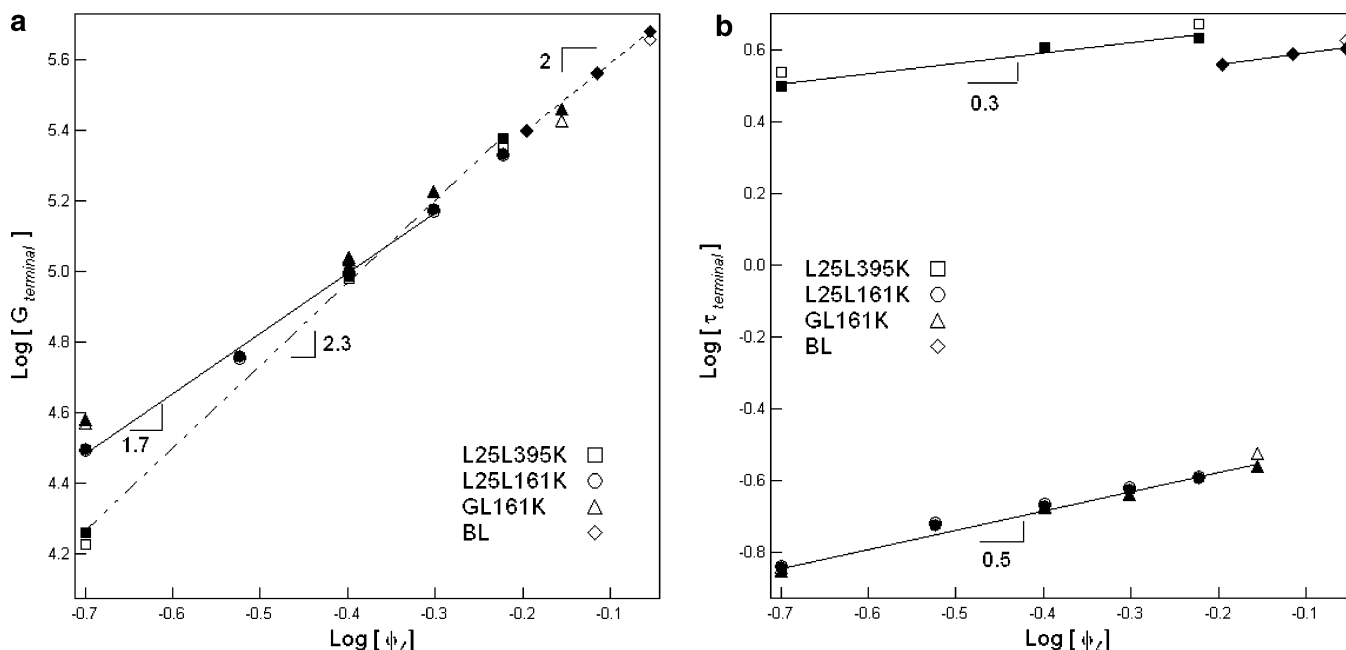
Figure 3. Terminal modulus and relaxation time vs volume fraction of long linear chains: (a) $G_{terminal}$ vs ϕ_l; (b) $\tau_{terminal}$ vs ϕ_l. The open symbols indicate terminal properties obtained using the extrapolation scheme described in the text and filled symbols indicate properties determined from the recoverable compliance J_{e0} and zero-shear viscosity η_0. Lines in the plot are best fits to the experimental data. Here BL identifies data for bidisperse linear blends from Rubinstein and Colby.[15]

blends to proceed by reptation diffusion of the long chains in a fully dilated tube. It is also apparent from the figure that two distinctive loss maxima and minima are observed for the linear/linear and star/linear blends. If we label the effective volume fraction of the slower relaxing component at the low-frequency plateau $\tilde{\phi}_l$ and again characterize the two rubbery regimes by the storage moduli G_I and G_{II} associated with the observed loss minima, then $\tilde{\phi}_l \approx (G_{II}/G_I)^{0.43}$ where the second plateau is taken to result from dilution of the network in which L395K relaxes. This simple analysis leads to $\tilde{\phi}_l \approx 0.49$ for GL395K50, $\tilde{\phi}_l \approx 0.62$ for L25L395K40, and $\tilde{\phi}_l \approx 0.42$ for L25L395K60. These values are in every case remarkably close to the overall volume fraction ϕ_l of the slower relaxing polymer blend component, confirming our assignment of G_{II} and that the faster relaxing component does in fact dilate the network in which the slower relaxing linear chains relax.

It is possible to roughly evaluate the importance of CR processes on terminal relaxation dynamics in linear/linear and star/linear blends from estimates of the terminal modulus and relaxation times of the blends. The terminal modulus $G_{terminal}$ and relaxation time $\tau_{terminal}$ are estimated using two different methods. In the first approach the $G_{terminal}$ is taken as the modulus and $\tau_{terminal}$ as the reciprocal frequency at which the extrapolated terminal moduli ($G'(\omega) \sim \omega^2$ and $G''(\omega) \sim \omega^1$) for the blends intersect. Values for $G_{terminal}$ and $\tau_{terminal}$ obtained in this way are plotted against ϕ_l in Figure 3 (open symbols). In the second approach the terminal properties are determined from the recoverable steady-state compliance $J_{e0} = \lim_{\omega \to 0} G'/|G^*|^2$ and the zero-shear viscosity η_0 using $G_{terminal} \approx J_{e0}^{-1}$ and $\tau_{terminal} \approx \eta_0 J_{e0}$. These values are also plotted against ϕ_l in Figure 3 (filled symbols). $G_{terminal}$ and $\tau_{terminal}$ estimates from published data for 1,4-polybutadiene linear/linear blends (BL: $M_l = 355000$, $M_s = 70\,900$)[15] are also included in the plots. Best-fit straight lines through the $\log(G_{terminal})$ vs $\log(\phi_l)$ plot support a scaling relationships $G_{terminal} \sim \phi_l^x$, with an exponent x of order 2. Figure

3b supports a similar scaling form $\tau_{terminal} \sim \phi_l^y$, with exponent y of order 0.5 for the L25L161K and GL161K blends and approximately 0.3 for the L25L395K and BL series blends.

With $M_e = \rho RT/(^5/_4)G_I = 1505$ g/mol for the 1,4-PBD melt, $z_t \geq 21$ and $G_r = 0.02$ for the L25L161K series, $z_t \geq 52$ and $G_r = 0.05$ for the L25L395K series, and $z_t \geq 150$ and $G_r = 0.002$ for BL series. On the basis of the criteria proposed by Doi et al.[8] and by Viovy et al.,[9] blends in all three series should be firmly in the "nondilated" category, in which $\tau_{terminal} \sim \phi_l^0$ and $G_{terminal} \sim \phi_l^2$. The case of terminal relaxation in a fully dilated tube on the other hand yield $\tau_{terminal} \sim \phi_l$ and $G_{terminal} \sim \phi_l^2$. We therefore tentatively conclude that terminal dynamics in both the linear/linear and star/linear blend systems studied here are intermediate between the two extremes considered above. Later we will show that it is possible to estimate the degree of tube enlargement at the terminal time using theory. These results indicate that the tube diameter increases by as little as 8% and at most 30% for the materials considered, perhaps explaining the weaker than expected concentration dependence of $\tau_{terminal}$. We also conclude that the parameters G_r and z_t are insufficient to establish what dynamic processes are dominant during terminal relaxation of the bidisperse linear blends used in this study. It is likely that omission of CLF contributions to the reptation relaxation times of long and short chains in the derivation of G_r, slowing down of short-chain dynamics in the presence of long chains, and the oversimplified form of the CR term, all play some role in the observed variability of G_{rc}.

A rigorous self-consistent theory for modeling stress relaxation dynamics in bidisperse linear blends was proposed sometime ago by Rubinstein and Colby.[15] This theory takes into account the local effect of constraint loss by modeling constraint release as a bead–spring Rouse chain with a random distribution of bead friction coefficients. It has been used to successfully model linear viscoelastic properties of binary linear/linear blends,[15]

but is not easily extended to star/linear blends. The MM model, like the Doi−Edwards model, is a single chain model derived by coarse graining the chains surrounding a test molecule into a uniform tube. To use this model for predicting stress relaxation dynamics in binary blends therefore requires a great deal of intuition/apriori knowledge about how local loss of constraints resulting from faster relaxation of one component in the blend affect the size of the tube and thereby the dynamics of the chain trapped in it. The strengths of this model is its simplicity and flexibility. It is quite straightforward, for example, to incorporate new physical processes to describe tube relaxation in blends. Used in conjunction with careful rheological measurements, the MM model therefore provides a useful tool for extracting microscopic information about the physical processes responsible for macroscopic rheological behavior. We will use the model in this way throughout the remainder of this article.

$G'(\omega)$ and $G''(\omega)$ data discussed in the last section will be employed to quantitatively evaluate predictions of the MM model suitably modified to account for the possible UDT, UDT wCR, and TD modes of relaxation. Similar detailed comparisons will be used to explore the molecular-scale physical processes by which short stars and linear chains alter dynamics of the long linear molecules in binary blends, as well as how the long chains in turn slow-down relaxation of the faster relaxing blend components. The model expressions used in our analysis are summarized in the Appendix. Only three model parameters are evidently necessary for the analysis, a plateau modulus G_N, entanglement molecular weight M_e, and an entanglement equilibration time τ_e. While the value of $M_e = \rho RT/G_e$ and $\tau_e = \zeta a^4/3\pi^2 k_B T b^2$ can be rigorously calculated from measured or literature values of the polymer density ρ, the tube diameter a, the monomer (Kuhn) length b, the monomeric friction coefficient ζ and the plateau modulus G_N, data for some parameters, e.g. ζ are not generally available at the conditions used for the experiments. Thus, in this article G_N, M_e, and τ_e are obtained by fitting the model expressions to the measured dynamic moduli for narrow molecular weight distribution linear PBD melts.

Figure 4a−d provides comparisons between experimental $G'(\omega)$ and $G''(\omega)$ with predictions of the MM-model. All model predictions use $G_{Nf} = 1.42$ MPa, $\tau_{ef} = 3 \times 10^{-7}$ s, and $M_{ef} = 1800$ g/mol, which are independently evaluated, rather calculated by the theoretical relationship $G_e = \rho RT/M_e = {}^5/_4 G_N$.[16] G_{Nf} is about 20% larger than the plateau modulus $G_I = 1.19(\pm 0.09)$ MPa estimated as the average storage modulus value at which the first rubbery loss minimum is observed. The best-fit entanglement molecular weight M_{ef} is also about 20% larger than the entanglement molecular weight $M_e = \rho RT/({}^5/_4)G_I = 1505$ g/mol calculated from G_I, with $T = 301$ K and $\rho = 0.895$ g/cm^3.[17] Parts a and b of Figure 4 show how the choice of model parameters affects the quality of the fits with the M_e and G_N relationship. While this independent fitting yields a higher value of $G_{ef}M_{ef} = {}^5/_4 G_{Nf}M_{ef}$ than the expected ρRT by 43%, the best-fit model parameters are in good agreement with parameters reported in our previous article on star/linear PBD blend dynamics.[7] The dilution exponent α is fixed to the theta solution value $\alpha = {}^4/_3$ because all polymers used in the blends are chemically identical and the lower molecular weight component large enough to expect theta solution properties.[7,11] $G'(\omega)$ and $G''(\omega)$ data

for all polymers used in the study are compared with the MM-model predictions in Figure 4, parts c and d. The same "best-fit" parameter values discussed above are used throughout.

It is evident from the plot that except for small discrepancies in the depth of the high-frequency loss minimum, $G'(\omega)$ and $G''(\omega)$ are quite well predicted for the higher molecular weight linear polymers. Significant quantitative discrepancies are nonetheless observed between theory and experiment for the two lowest molecular weight polymers L25 and GYS. Furthermore, in the case of GYS the arm molecular weight used in the theoretical analysis, and for all subsequent comparisons in this paper, had to be adjusted upward to $M_{a,GYS} = 11\,500$ g/mol. This value is about 25% larger than the arm molecular weight estimated from the overall molecular weight of the 4-arm star determined from static light scattering measurements $M_{GYS} = 36\,300$ g/mol and about 15% larger than the arm molecular weight determined from SEC analysis, to correctly reproduce the experimental crossover frequency. It is possible that this discrepancy in arm molecular weight could in reality arise from slight differences in M_e for the star and linear PBD chains; however, NMR analysis indicates (see Table 1) that their microstructures are essentially identical, which rules out this possibility. Other sources of experimental error arising, for example, from the inherent difficulty in performing SEC and static light scattering measurements on low molecular weight polymers cannot be ruled out. It is nonetheless clear from Figure 4d that even with the higher value of $M_{a,GYS}$, the theory only qualitatively captures the experimental $G'(\omega)$ and $G''(\omega)$ trends for GYS and L25K, indicating that the discrepancy in molecular weights may well reflect shortcomings of the theory when applied to such low molecular weight entangled polymers as used here.

$G'(\omega)$ and $G''(\omega)$ data for L25L161K50 are compared with the model predictions in Figure 5a. Predictions obtained under assumption 3 (TD mode) clearly provide the best description of the experimental results over the broadest frequency range. Even though small discrepancies between the theoretical and measured moduli are observed in places, the agreement is very good. It is important to notice that if only the terminal region ($\omega < 10^2$) is compared, predictions assuming terminal relaxation of the longer chains occurs in an undilated tube at a faster rate than CR motion (UDT mode) are seen to be comparable to those for the TD mode. However, the moduli predicted under the UDT assumption significantly underestimates the loss modulus in the low-frequency dynamic regime just prior to where $G''(\omega)$ exhibits a local maximum (believed to be related to the relaxation of the shorter linear chains). Predictions based on the (UDT wCR mode) amends these results, but yields much too slow terminal relaxation. These observations demonstrate that contrary to expectations based on G_r and on our earlier analysis of terminal properties of linear/linear blends, the longer linear chains in the L25L161K50 blend relax by reptation diffusion in a fully dilated tube. This conclusion is supported by results in Figure 5b where the theory is seen to semiquantitatively capture blend dynamics in three different linear/linear polymer blend systems, all under the assumption that terminal dynamics of the slower relaxing molecules proceeds by reptation diffusion in a fully dilated tube.
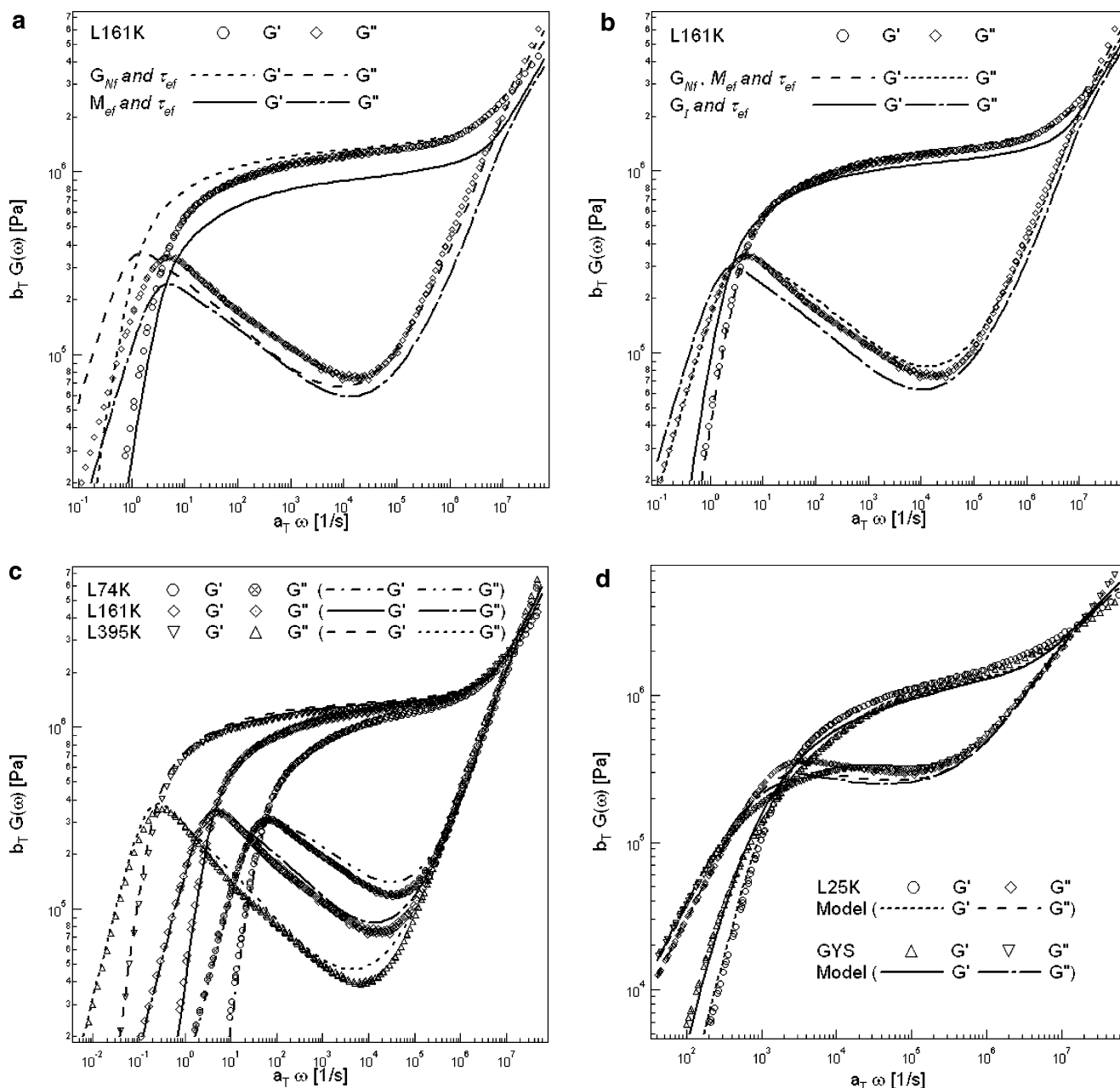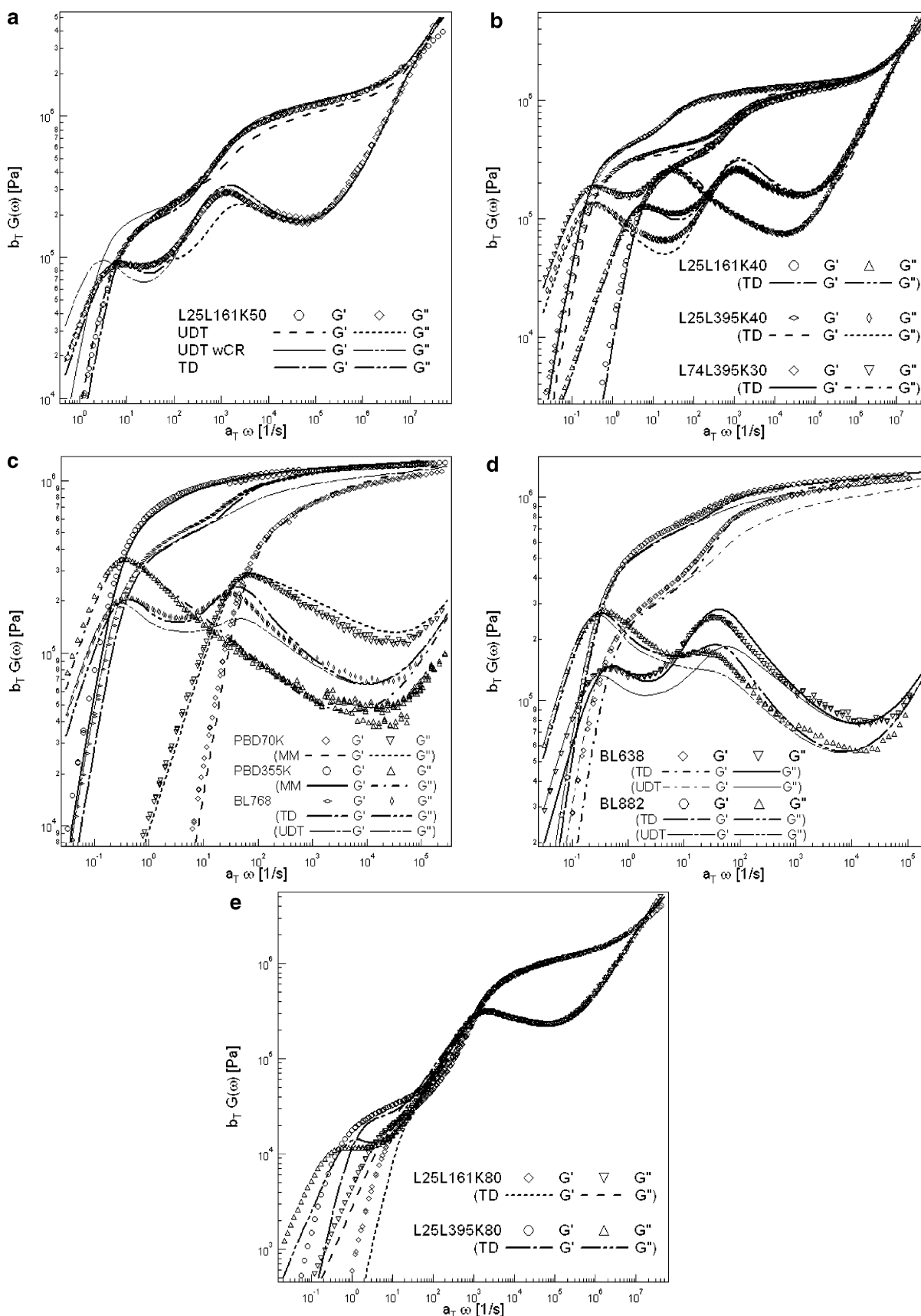
Figure 4. Comparisons of experimental and theoretical moduli, $G'(\omega)$ and $G''(\omega)$, for 1,4-polybutadiene: (a) linear polymers (L161K) with two best-fit parameters, (b) linear polymers (L161K) with three best-fit parameters and the measured plateau modulus and τ_{ef}, (c) long linear polymers (with G_{Nf}, M_{ef} and τ_{ef}) and (d) short linear and short arm star polymer melts (with G_{Nf}, M_{ef}, and τ_{ef}) using the model of Milner and McLeish[1,2] with $\alpha = {}^4/_3$. The reference temperature is 28 °C. Model parameters used for these comparisons are provided in the text.

Our finding that dynamic tube dilation is competitive with reptation in an undilated tube is not surprising on physical grounds for blends where the terminal times for the slow- and fast-relaxing components are well separated. This finding is nonetheless at odds with expectations based on early scaling models,[8,9] which predict that terminal dynamics in all linear/linear blends studied so far should be dominated by reptation diffusion of the long chains in undilated tubes. It is also inconsistent with our analysis based on terminal properties ($G_{terminal}$ and $\tau_{terminal}$), which point to the more complex scenario of reptation diffusion in a partially dilated tube. Sometime ago Rubinstein and Colby[15] studied stress relaxation in bidisperse of long linear, M_l = 355000 g/mol and short linear, M_s = 70900 g/mol, 1,4-polybutadiene molecules. Blends with long chain volume fractions ϕ_l of 0.638, 0.768, and 0.882 are designated BL638, BL768, and BL882 (BL series). The ratio of long and short polymer component molecular weight in these blends is comparable to the L74L395K30 PBD blend in Figure 5b, where predictions based on the TD scenario are in nearly quantitative agreement with the experimental data.

Parts c and d of Figure 5 compare experimental data and theoretical predictions of $G'(\omega)$ and $G''(\omega)$ for the BL series blends and the corresponding pure components. But for the fact that G_{Nf} used in the analysis is 10% lower than the value used earlier for the pure PBD polymers and their blends, the MM-model reproduces the experimental $G'(\omega)$ and $G''(\omega)$ data for the pure components with the same parameters used earlier to analyze the PBD systems. Using these same parameters

Figure 5. Comparisons of experimental and theoretical moduli, $G'(\omega)$ and $G''(\omega)$: (a) for a blend of short linear (L25K) and long linear (L161K) polymers at $\phi_l = 0.5$ at $T_{Ref} = 28$ °C, (b) for linear/linear blends with variable short and long polymer molecular weights and volume fractions, L25L161K40 with $\phi_l = 0.6$, L25L395K40 with $\phi_l = 0.6$ and L74L395K30 with $\phi_l = 0.7$, at $T_{Ref} = 28$ °C, (c) for short linear (PBD70K), long linear (PBD355K) melts, and a blend with $\phi_l = 0.768$ (BL768) at $T = 30$ °C from Rubinstein and Colby[15], (d) for blends of short linear (PBD70K) and long linear (PBD355K) polymer with $\phi_l = 0.638$ (BL638) and 0.882 (BL882) at $T = 30$ °C from Rubinstein and Colby,[15] and (e) for linear/linear blends with $\phi_l = 0.2$, L25L161K80 and L25L395K80, at $T_{Ref} = 28$ °C. Lines are model predictions described in the Appendix.
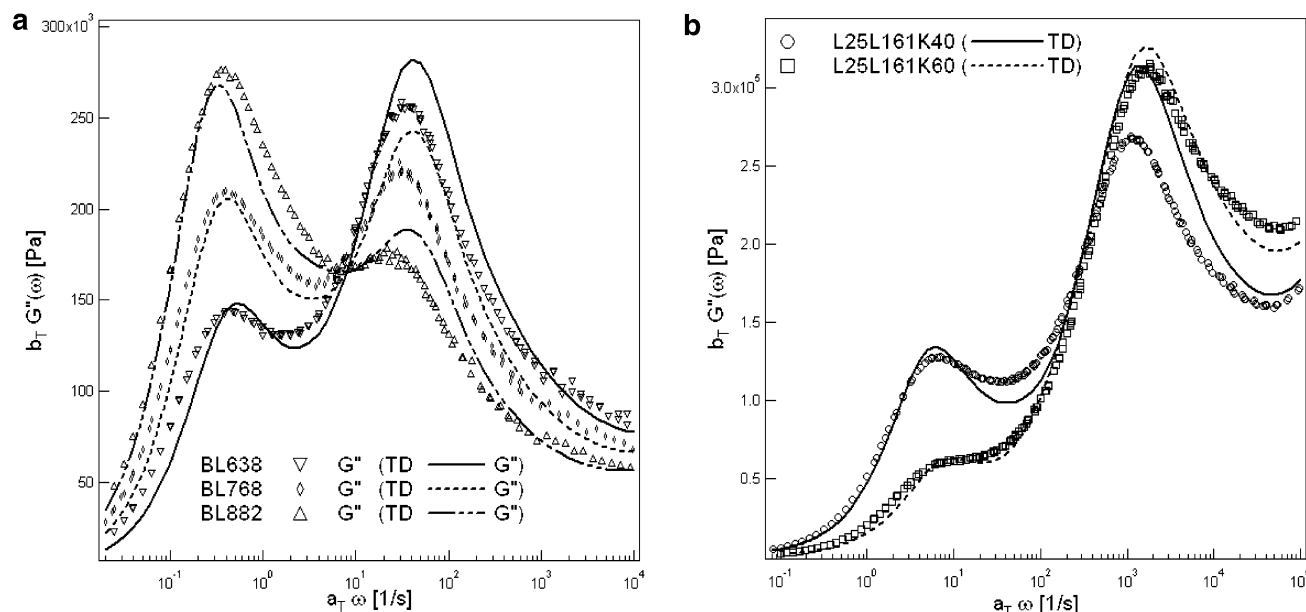
Figure 6. Comparison of experimental and theoretical loss modulus, $G''(\omega)$: (a) for blends of short linear (PBD70K) and long linear (PBD355K) polymers, BL series, with $\phi_l = 0.638$, 0.768, and 0.882 at $T = 30$ °C from Rubinstein and Colby[15] and (b) for linear/linear blends with $\phi_l = 0.6$ (L25L161K40) and $\phi_l = 0.4$ (L25L161K60) at $T_{Ref} = 28$ °C. Lines are the model predictions of TD mode described in the Appendix.

we compare $G'(\omega)$ and $G''(\omega)$ data with theoretical predictions based on the TD and UDT scenarios. It is evident from Figure 5, parts c and d that while some quantities like the $G''(\omega)$ maximum and minimum are not perfectly predicted, the TD physics again provide the most complete description of dynamics over the entire frequency range studied.

Given the aforementioned weak dependence of the experimentally determined terminal time on the long chain concentration in the blends, it is instructive to inquire how dilated the tube really is during terminal relaxation. To answer this question we determine $\beta = a_{eff,TD}/a_{eff,UTD}$ at the terminal time using the theory. For the blend L25L161K50 this analysis yields $\beta = 1.28$, and $\beta = 1.21$, 1.31, and 1.24 for L25L161K40, L25L395K40, and L74L395K30, respectively. In the case of the BL-series blends, $\beta = 1.08$, 1.18, and 1.3 with decreasing ϕ_l. Thus, the tube diameter is dilated by at most 30% during terminal relaxation of these materials.

On the basis of Figure 5a−d, it is tempting to conclude that the TD model provides a satisfactory reproduction of dynamics in bidisperse linear polymer blends comprised of components with well separated terminal relaxation times. The quality of the predictions also appear to be only weakly sensitive to the relative molecular weight of the two linear polymers, which is also a desirable result. This situation contrasts with the results summarized in Figure 5e where the volume fraction of the long molecules is deliberately chosen so that the shorter linear chains are themselves unconstrained by the dilated tube. This situation is arguably the most straightforward, since terminal dynamics might be expected to be analogous to those in a neat entangled solution of the long linear polymer. Figure 5e nonetheless shows that while the model predictions based on TD mode terminal relaxation is in quantitative accord with the experimental data at high frequency, $G'(\omega)$ and $G''(\omega)$ are only captured qualitatively at intermediate and low frequencies. Predictions based on the other two relaxation modes are, as expected, worse. We suspect that the discrepancy between the TD mode

calculations and the experimental results is related to a similar breakdown of the MM-model for entangled polymer solutions at low polymer concentration. Here again the theory predicts faster than expected terminal relaxation, but also underpredicts the plateau modulus. The fundamental source of these effects is not yet understood.

Parts a and b of Figure 6 provide more revealing comparisons of the experimental and theoretical loss moduli for the BL series and the L25L161K series blends by plotting $G''(\omega)$ on a linear scale. It is evident from both figures that while the TD-based model provides a reasonable qualitative account of dynamics in the blends, significant discrepancies exist particularly near the high frequency loss maxima associated with relaxation of the lower molecular weight chains. Thus, while the BL series blends show a small, but noticeable slowing down of the shorter chain relaxation dynamics with increasing concentration of the higher molecular weight molecules, the theory shows no noticeable change in the position of the high frequency loss maxima. A mechanism for such slowing down exists in the MM-model; i.e., the slower relaxing long chains provide an effective permanent network that retards short-time CLF relaxation dynamics of the short chains, the effect is hardly noticeable, however, for the BL series polymers. In the case of the shorter L25 chains, slower relaxation of the shorter chains is observed, both from experiment and theory, as the long chain concentration is increased. The effect is nonetheless still not fully captured by the MM-theory.

The predictions shown in Figure 6a are of comparable quality to results reported by Rubinstein and Colby (see Figure 6b of ref 15), using their self-consistent model for constraint release, and by Frischknecht and Milner (Figure 2b in ref 18), based on an approximate form of the model used here with the assumption that the UDT wCR mode dominates terminal relaxation dynamics. The predicted magnitude of $G''(\omega)$ peak and the frequency of the $G''(\omega)$ maximum of long chains based on
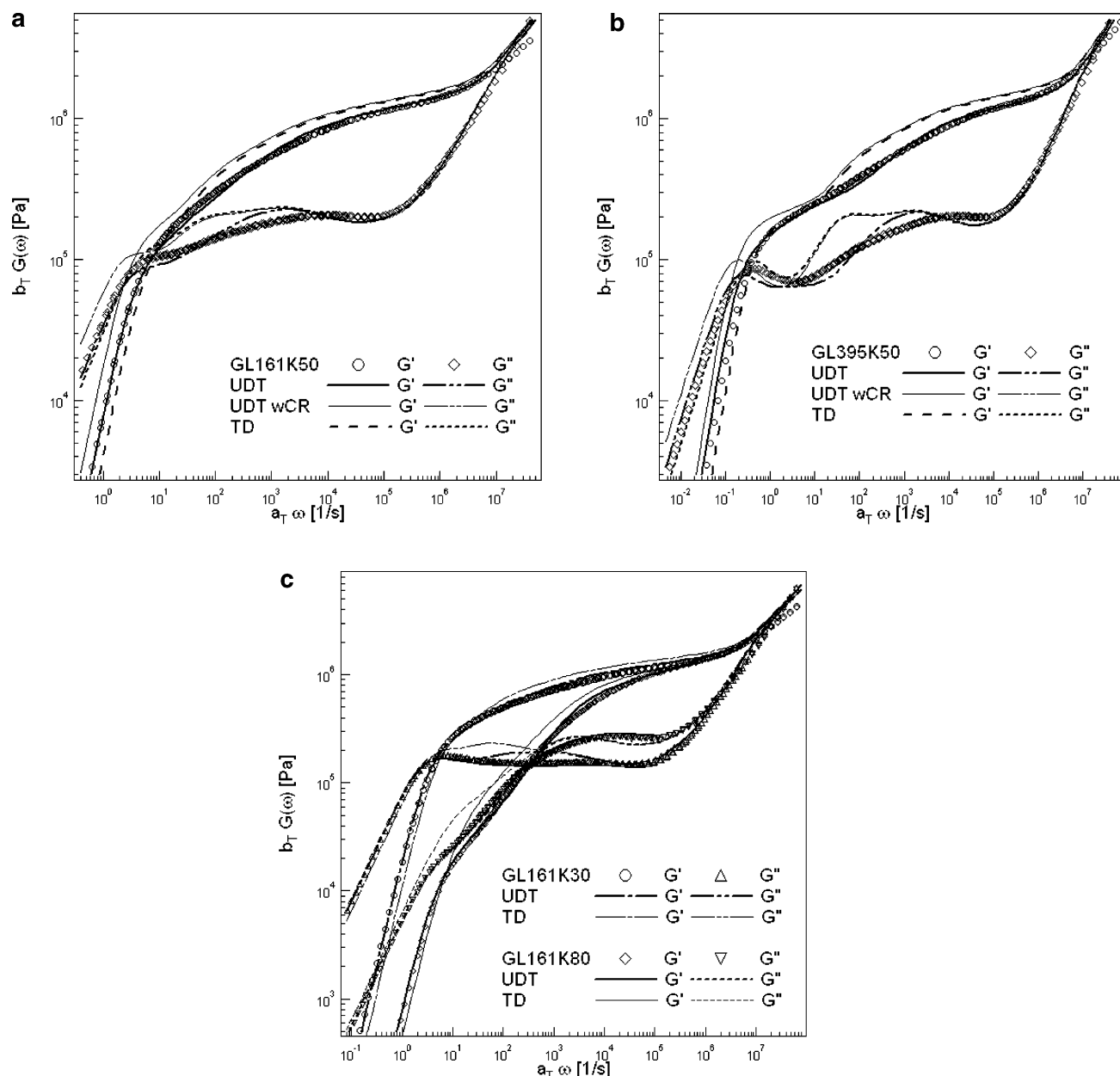
Figure 7. Experimental and theoretical moduli, $G'(\omega)$ and $G''(\omega)$: (a) for a blend of short arm star (GYS) and long linear (L161K) polymers with $\phi_l = 0.5$ (GL161K50), (b) for a blend of short arm star (GYS) and long linear (L395K) polymers with $\phi_l = 0.5$ (GL395K50), and (c) for blends of short arm star (GYS) and long linear (L161K) polymers with $\phi_l = 0.7$ (GL161K30) and $\phi_l = 0.2$ (GL161K80). The reference temperature is 28 °C. Lines are the model predictions.

the TD mode are nonetheless seen to be closer to the measured BL-series data than those of the two earlier studies.[15,18] The largest deviations in all three studies appears in the $G''(\omega)$ peak associated with the faster relaxing chains. Predictions based on the dilated tube assumption (TD mode) overestimates the magnitude of the $G''(\omega)$ peak, while those based on the UDT mode severely underestimates it. The only available theory that appears to quantitatively reproduce both loss maxima is the theory of Pattamaprom et al.[19] This theory uses an ad hoc dual constraint model that combines double reptation and tube dilution ideas; again suggesting that physics intermediate between the TD and UDT relaxation modes are required to quantitatively capture the underlying dynamics in binary linear/linear blend systems.

To examine the waiting process in binary blends (i.e., period between the end of short chain relaxation and equilibration of the longer chains in a dilated tube), we

now turn to a more detailed analysis of terminal relaxation dynamics in short star/linear blends. Figure 7a compares model predictions for each of the three terminal modes with the measured moduli for GL161-K50. The overall agreements between predicted and measured storage $G'(\omega)$ and loss $G''(\omega)$ are clearly not as good as for the linear/linear blends with similar volume fraction of long chains. The weak $G''(\omega)$ maximum related to relaxation of the star is, for example, only qualitatively captured by the model. Predictions based on the TD and UDT wCR terminal modes overestimate $G'(\omega)$ in both plateau regions and result in a significant delay of the loss maximum. On the other hand, predictions based on the UDT mode qualitatively capture much of the dynamics reported in $G'(\omega)$ and $G''(\omega)$, including a slight kink between the $G''(\omega)$ maximum and the $G'(\omega)-G''(\omega)$ crossover point. The position of the loss maximum is nonetheless delayed relative to where it is seen experimentally, which may

be a consequence of the already demonstrated difficulty the model encounters in predicting relaxation of the GYS melt. At the crossover frequency, both moduli are also predicted to be lower than observed from experiment.

$G'(\omega)$ and $G''(\omega)$ for a star/linear blend with higher linear polymer molecular weight (GL395K50) are presented in Figure 7b. The experimental data are again compared with model predictions under the three scenarios discussed in the Introduction. Despite the now quite prominent secondary loss minimum and the fact that $(G_{II}/G_I)^{0.43} = \bar{\phi}_l \approx 0.49$ is the result expected if terminal relaxation of the linear chains occurs in a network dilated by the relaxed stars, the UDT mode is again observed to best describe dynamics in the blends. Only a weak hint of a second loss maximum is evident in Figure 7a, but even in that case we find $(G_{II}/G_I)^{0.43} = \bar{\phi}_l \approx 0.495$ for GL161K50. Figure 7c provides additional comparisons for star/linear blends with majority linear (GL161K30) and star (GL161K80) polymer. Again the predictions are not quantitative, but those based on terminal relaxation of the long linear chains in an undilated tube best capture the actual blend dynamics. Thus, unlike linear/linear blends, where terminal relaxation of the slower relaxing component occurs by reptation in a dilated tube, reptation in an undilated tube consistently captures terminal relaxation of long linear chains in the short star/linear blends. This observation may seem surprising given the closeness of the experimentally determined $\tau_{terminal}$ values of star/linear and linear/linear blends (see Figure 3b). However, as shown earlier the tube dilation produces only a modest change in the terminal tube diameter (less than 30%) in the linear/linear blends. This means that the terminal time computed using either UDT or TD modes will be quite similar (see Figure 7). It is nonetheless clear from the plateau modulus results that the relaxed stars do enlarge/perforate the network in which the long linear chains reptate.

Together these results indicate that the relaxed star arms do release constraints on the long linear chains, but the tube equilibration process needed for the linear chains to take advantage of the looser network to accelerate molecular relaxation is influenced by the short chain architecture. This picture of constraint release whereby the polymer chains that initiate the release can also influence how the partner chain takes advantage of its new surroundings is intuitive, but has not yet been described mathematically. It is also quite different from constraint release processes described in the literature[8,9] and hence requires further investigation. These findings are also probably related to recent observations for multiarm/pompom $A_3-\mathbf{A}-A_3$ polymers, which also show a second loss plateau following relaxation of the entangled A arms consistent with dilution of the network environment in which the cross-bar $\mathbf{A}$ relaxes, yet terminal dynamics of the cross-bar are best described as reptation diffusion in the original/undilated tube.[20]

An alternative explanation of the star/linear blend results is that the long linear chains slow-down relaxation of the short stars to such an extent that entanglement constraints produced by the stars are much longer-lived than anticipated from the terminal time of the pure star polymer. The model outlined in the Appendix accounts for the possibility of frustrated dynamic dilution of the faster relaxing star arms by the more slowly

relaxing linear chains. It can therefore be used to quantify slowing-down of star polymer relaxation in short star/linear blends. For the blends GL395K50 and GL161K50 the arm retraction time is predicted to increase by factors of 4.8 and 3.7, respectively. For GL161K30 and GL161K80 the retraction time in the blend increases by factors of 6.2 and 1.8, respectively. Given the already large difference in average relaxation times of the pure polymers $\bar{\tau}_{L395K}/\bar{\tau}_{GYS} \sim 3600$ and $\bar{\tau}_{L161K}/\bar{\tau}_{GYS} \sim 212$, even these levels of retarded relaxation of the stars cannot fully explain the qualitative differences between the short stars and short linear chains on terminal relaxation dynamics in the blends.

All of the short star/linear blend work discussed in the article so far are based on results from a single star PBD (GYS). A source of concern is that there may be something unusual about this material that escapes detection by the experimental methods used to characterize it. We therefore synthesized a model 3-arm star polyisoprene (PI) and several linear PIs using anionic procedures described in the Experimental Section. Because of the larger entanglement molecular weight of PI it is more difficult to synthesize narrow distribution star and linear polymers with as wide a separation of terminal times as in the PBD systems. For brevity we focus on blends of a single short star (S) and linear PI (N250K, see Table 1) with variable blend composition. The ratio of terminal times for the pure polymers is $\bar{\tau}_{N250K}/\bar{\tau}_S \sim 46$.

As in the case of PBD, model parameters of PI were obtained by fitting the melt rheology data to the MM-model. Figure 8a illustrates the quality of the fits. It is evident from the figure that $G'(\omega)$ and $G''(\omega)$ for both materials are qualitatively reproduced by the model, but there are small quantitative discrepancies at several places in the spectrum. In this case the dynamic storage and loss moduli of the star polymer are evidently more accurately captured by the model. The model parameters used in this analysis are $G_{Nf} = 0.6$ MPa, $\tau_{ef} = 7.4 \times 10^{-6}$ s, and $M_{ef} = 4200$ g/mol, compared with $G_N = 0.42(\pm 0.03)$ MPa estimated from the storage modulus at the loss minimum and $M_e = 4290$ g/mol calculated from G_N with $T = 301$K and $\rho = 0.9$ g/cm^3.[17] The best-fit parameters are again independently evaluated using different linear PI polymers and the product of the best-fit $G_{ef}(= {}^5/_4 G_{Nf})$ and M_{ef} parameters is higher than the theoretical value of ρRT by 40%. As shown in Table 1, the average molecular weight of the linear PI required to reproduce the crossover frequency and terminal dynamics is 9% larger than the average molecular weight determined from light scattering.

Model predictions based on terminal relaxation of the slower relaxing linear chains by TD and UDT modes are compared with the experimental data for SN250K series star/linear blends with variable ϕ_{N250K} in Figure 8, parts b and c. The overall quality of the predictions are not as good as in the case of the PBD blend systems; a perhaps obvious carryover from the pure melt results. However the predictions provided under the assumption that terminal dynamics of the linear chains occur in an undilated tube are again found to be consistently superior to those obtained assuming the relaxed star uniformly dilates the tube in which the longer linear chains reptate. This last finding is consistent with our previous observations for the PBD systems and serves to reiterate the fact that both phases of constraint release (constraint loss and tube equilibration) are
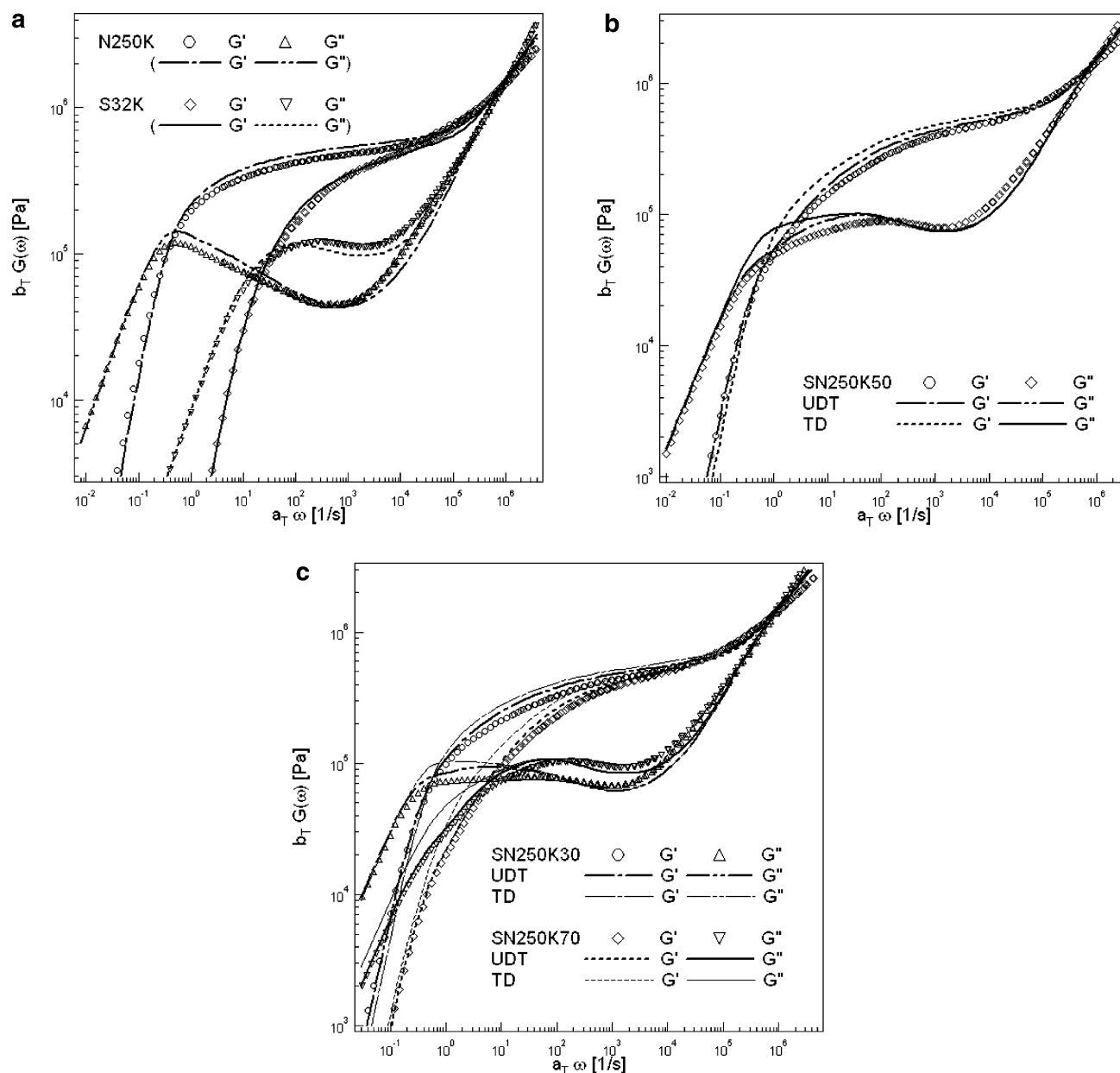
Figure 8. Experimental and theoretical moduli, $G'(\omega)$ and $G''(\omega)$: (a) for 1,4-polyisoprene short arm star (S32K) and long linear (N250K) polymer melts using the Milner–McLeish model[1,2] with $\alpha = {}^4/_3$. Parameters used for these comparisons are provided in the text; (b) for a blend of short arm star (S32K) and long linear (N250K) polymers at $\phi_l = 0.5$ (SN250K50), and (c) for blends of short arm star (S32K) and long linear (N250K) polyisoprene with $\phi_l = 0.7$ (SN250K30) and $\phi_l = 0.3$ (SN250K70). The reference temperature is 28 °C. Lines are the model predictions.

influenced by the architecture/detailed dynamics of the faster-relaxing/leaving chains.

Exactly how this effect can be taken into account to refine the current picture that tube-in-supertube Rouse dynamics defines the final stage of constraint release in blends remains an open question. Again, we can calculate the effect of slower relaxing linear chains on the retraction time for the stars. For SN250K30 the arm retraction time in the blend is estimated to be larger by a factor of 6.4; for SN250K50 and SN250K70 it is larger by factors of 3.8 and 2.4, respectively. While it is possible that such slowing-down of arm retraction dynamics in the SN250K30 blend can account for the unexpected, long-lived influence of short PI stars on the linear polymer dynamics, this effect cannot in of itself explain relaxation dynamics of the SN250K50 and SN250K30 blends. It is of course possible that the high

spatial density of segments belonging to a single short star polymer leads to longer-lived topological constraints, which delay access to the larger supertube created by relaxation of star arms. Indeed while it only takes a time of order the terminal time for all segments of a linear molecule to diffuse away from a partner chain, segments of a star may require a much larger time (of order $\sqrt{N_a/N_e}\tau_a$) to entirely release an entangled partner. This effect is not taken into account by any of the current theories for stress relaxation in star/linear and star/star blends, it will be investigated in greater detail in future work.

Conclusion

Stress relaxation dynamics in a series of linear/linear and short arm star/linear blends were studied using oscillatory shear flow measurements. To investigate

constraint-release and tube dynamics, dynamic storage, $G'(\omega)$, and loss, $G''(\omega)$, moduli were directly compared with predictions of a version of the tube model proposed by Milner and McLeish (MM-model). While the relaxation dynamics of linear/linear blends are reasonably described by the MM-model predictions assuming terminal relaxation of the slower relaxing linear chains occurs by reptation diffusion in a dilated tube, the predictions suggest that long linear chains blended with short entangled star polymers relax by reptation diffusion in an undilated tube. This finding is on its surface inconsistent with our observation that faster relaxing linear and star chains have the same effect on the shear modulus of these same blends. Specifically, following relaxation of short star and linear chains in the blends a second plateau region is observed with modulus G_{II} related to the plateau modulus, G_I, in the rubbery plateau by $(G_{II}/G_I)^{0.43} = \phi_l$, where ϕ_l is the volume fraction of long linear chains in the blends. A more careful assessment of these results, however, indicates that tube dynamics in the presence of relaxed star molecules are fundamentally different than for linear chains. While it is clear that the relaxed star arms do release constraints on the long linear chains, the tube equilibration process needed for the linear chains to take advantage of the looser network to accelerate molecular relaxation is slowed-down by the star molecules.

Appendix

The Milner−McLeish star/linear blend framework[6] was extended to model dynamics in blends of short linear chains and short star molecules in long linear hosts. Recent numerical correction factors introduced by Likhtman and McLeish[16] as well as the more accurate value of the dilution exponent α[7,11] are included in the model used in this work. The same physical picture of constraint-release (CR) tube Rouse motion developed in refs 6 and 7 is applied to the relaxation dynamics of long linear polymers in these blends. The number of entanglement segments of short linear polymer Z_S, long linear polymer Z_L and star arm Z_a are defined as $Z_S = M_sM_e = (M_s/M_0)/(M_e/M_0)$, $Z_L = N_l/N_e$ and $Z_a = N_a/N_e$, respectively, where M_0 is the monomer molecular weight and M_e is the entanglement molecular weight. τ_e is the equilibration time for the entanglement strand, s_i is defined as the fractional distance from the end of arm, where linear polymers are regarded as two-arm stars, and ϕ_i is weight fraction of each polymer in the blend. The subscripts i indicate long linear ($i = l$), short linear ($i = s$) and short arm star polymers ($i = a$).

A. Short Star/Long Linear Blends. In the fluctuation (starlike retraction) regime, the effective fraction of unrelaxed segments $\Phi(s_i)$ and the effective potential $U_{i,b}(s_i)$ for short star/long linear blends are defined

as follows:

$$\Phi(s_l) = 1 - \underline{VF_l}\,s_l = 1 - \left(\phi_l + \phi_a\sqrt{\frac{Z_L}{2Z_a}}\right)s_i \quad (A1)$$

$$\Phi(s_a) = 1 - \underline{VF_a}\,s_a = 1 - \left(\phi_a + \phi_l\sqrt{\frac{2Z_a}{Z_L}}\right)s_a \quad (A2)$$

$$U_{l,b}(s_l) = 3\frac{Z_L}{2}\frac{1 - (1 - VF_ls_l)^{\alpha+1}[1 + (1 + \alpha)VF_ls_l]}{VF_l^{\,2}(1 + \alpha)(2 + \alpha)} \quad (A3)$$

$$U_{a,b}(s_a) = 3Z_a\frac{1 - (1 - VF_as_a)^{\alpha+1}[1 + (1 + \alpha)VF_as_a]}{VF_a^{\,2}(1 + \alpha)(2 + \alpha)} \quad (A4)$$

Here, the effective fraction of unrelaxed segments $\Phi(s_i)$ is expressed in terms of the fractional distance s_i with the factor VF_i derived from the Ball−McLeish equation.[6,7,21]

The *early fast diffusion* time of linear and star polymers[1,2] is given by

$$\tau_{\text{early}}(s_l) = \frac{9\pi^3}{16}\tau_e\left[\frac{Z_L}{2}\right]^4 s_l^{\,4} \quad (A5)$$

$$\tau_{\text{early}}(s_a) = \frac{9\pi^3}{16}\tau_e Z_a^{\,4} s_a^{\,4} \quad (A6)$$

The *late diffusion* time of star and linear polymers is given by[2,6,7,21]

$$\tau_{\text{late}}(s_l) = \sqrt{\frac{\pi^5}{6}\tau_e}\left[\frac{Z_L}{2}\right]^{3/2} \times$$
$$\frac{\exp[U_{l,b}(s_l)]}{\sqrt{s_l^{\,2}(1 - VF_ls_l)^{2\alpha} + \frac{1}{VF_l^{\,2}}\left(\frac{VF_l^{\,2}(1 + \alpha)}{3(Z_L/2)}\right)^{2\alpha/(1+\alpha)}\left(\Gamma\left[\frac{1}{1 + \alpha}\right]\right)^{-2}}} \quad (A7)$$

$$\tau_{\text{late}}(s_a) = \sqrt{\frac{\pi^5}{6}\tau_e}[Z_a]^{3/2} \times$$
$$\frac{\exp[U_{a,b}(s_a)]}{\sqrt{s_a^{\,2}(1 - VF_as_a)^{2\alpha} + \frac{1}{VF_a^{\,2}}\left(\frac{VF_a^{\,2}(1 + \alpha)}{3Z_a}\right)^{2\alpha/(1+\alpha)}\left(\Gamma\left[\frac{1}{1 + \alpha}\right]\right)^{-2}}} \quad (A8)$$

The combined retraction time $\tau_{i,b}(s_i)$ is defined as[2,6,7]

$$\tau_{i,b}(s_i) = \frac{\tau_{\text{early}}(s_i)\,\exp[U_{i,b}(s_i)]}{1 + \exp[U_{i,b}(s_i)]\tau_{\text{early}}(s_i)/\tau_{\text{late}}(s_i)} \quad (A9)$$

Therefore, the terminal relaxation time of short arm star in the blend is $\tau_{a,b}(s_a = 1) = \tau_a$.[2,21,22]

A1. Reptation of Unrelaxed Sections of Long Linear Polymers in the Dilated Tube. TD. After relaxation of star polymers, the position of the first unrelaxed long chain segment, s_{TD}, is determined by solving $\tau_a = \tau_{l,b}(s')$. At this time, the effective fraction of unrelaxed segments, abruptly reduces from $\Phi(\tau_a) = \Phi(s_{TD})$ to $\phi_l(1 - s_{TD})$. Thus, the tube constraining unrelaxed sections of the long chains explores the enlarged tube (super-tube), determined from the unre-

laxed fraction $\phi_l(1 - s_{TD})$, by Rouse-like motions. This constraint-release tube Rouse motion ends when the effective unrelaxed fraction at time t becomes the unrelaxed fraction $\phi_l(1 - s_{TD})$. Here, the effective unrelaxed fraction at time t, $\Phi(t)$, and the constraint-release Rouse time, τ_C, are defined as follows:[6]

$$\Phi(t)^\alpha = \Phi(s_{\text{TD}})^\alpha \sqrt{\frac{\tau_a}{t}} \qquad (A10)$$

$$\tau_C = \tau_a \left(\frac{\Phi(s_{\text{TD}})}{\phi_l(1 - s_{\text{TD}})}\right)^{2\alpha} \qquad (A11)$$

If relaxation of unrelaxed long chain segments is assumed to be frozen during the time where CR equilibration is active, the long chain will recognize the increased entanglement spacing on a time scale of order τ_C. Therefore, further relaxation will be governed by the diluted entanglement equilibrium time $\tau_{e,D} = \tau_e/\phi_l^{2\alpha}$ with the number of entanglement segments $Z_{LD} = M_I/M_{e,D}$ determined from a simple modification of the diluted entanglement spacing $M_{e,D} = M_e/\phi_l^\alpha$.[2] Taking $\alpha = 4/3$, the combined retraction time, $\tau_{l,Sol}(s_l)$, can be expressed as equation (A15), in analogy with eq A9, with the diluted effective potential, i.e. the *early* and *late diffusion* times using the diluted entanglement molecular weight.

$$U_{l,Sol}(s_l) = 3\frac{Z_{LD}}{2}\frac{1 - (1 - s_l)^{\alpha+1}[1 + (1 + \alpha)s_l]}{(1 + \alpha)(2 + \alpha)} \qquad (A12)$$

$$\tau_{\text{early},Sol}(s_l) = \frac{9\pi^3}{16}\tau_{e,D}\left[\frac{Z_{LD}}{2}\right]^4 s_l^4 \qquad (A13)$$

$$\tau_{\text{early},Sol}(s_l) = \sqrt{\frac{\pi^5}{6}}\tau_{e,D}\left[\frac{Z_{LD}}{2}\right]^{3/2}$$
$$\frac{\exp[U_{l,Sol}(s_l)]}{\sqrt{s_l^2(1 - s_l)^{2\alpha} + \left(\frac{(1 + \alpha)}{3(Z_{LD}/2)}\right)^{2\alpha/(1+\alpha)}\left(\Gamma\left[\frac{1}{1 + \alpha}\right]\right)^{-2}}} \qquad (A14)$$

$$\tau_{l,Sol}(s_l) = \frac{\tau_{\text{early},Sol}(s_l)\exp[U_{l,\text{sol}}(s_i)]}{1 + \exp[U_{l,\text{sol}}(s_i)]\tau_{\text{early},Sol}(s_l)/\tau_{\text{late},Sol}(s_l)} \qquad (A15)$$

The reptation time of the effective linear polymer solution with the number of entanglement segments $Z_{LD} = M_I/M_{e,D}$ can therefore be expressed as

$$\tau_{d,Sol}(s_l') = 3\tau_{e,D}Z_{LD}^3(1 - s_l')^2 \qquad (A16)$$

On the other hand, the reptation time of linear polymer in the original (undilated) tube is

$$\tau_d(s_l') = 3\tau_e Z_L^3(1 - s_l')^2 \qquad (A16^*)$$

To maintain the continuity of relaxation times after the constraint-release Rouse regime, the combined retraction time after CR motion ($\tau_{l,TD}(s_l)$) is written in terms of τ_C.[6,7]

$$\tau_{l,\text{TD}}(s_l) = \tau_C\frac{\tau_{l,Sol}(s_l)}{\tau_{l,Sol}(s_{\text{TD}})} \qquad (A17)$$

The reptation time of the unrelaxed section of the long

linear chain in the dilated tube $\tau_{d,TD}$ is determined from the crossover time between the time scales for CLF and reptation in the dilated tube, (A17) and (A16), respectively. So $\tau_{d,TD}$ is $\tau_{d,Sol}(s_{f,TD})$ with $s_{f,TD}$ satisfying $\tau_{d,Sol}(s_l') = \tau_{l,TD}(s_l')$.

The full expression for $G(\omega)$ with $G_e = (5/4)G_N$ is then as follows:[1,2,6,16]

$$G(\omega) =$$

$$G_e\,\phi_a\left(\frac{1}{5Z_a}\sum_{p=1}^{Z_a-1}\frac{i\omega\tau_e Z_a^2}{p^2 + i\omega\tau_e Z_a^2} + \frac{1}{Z_a}\sum_{p=Z_a}^{N_a}\frac{i\omega\tau_e Z_a^2}{2p^2 + i\omega\tau_e Z_a^2}\right):$$
$$\text{Rouse of arm at high } \omega \quad (A18a)$$

$$+ G_e\,\phi_l\left(\frac{1}{5Z_L}\sum_{p=1}^{Z_L-1}\frac{i\omega\tau_e Z_L^2}{p^2 + i\omega\tau_e Z_L^2} + \frac{1}{Z_L}\sum_{p=Z_L}^{N_L}\frac{i\omega\tau_e Z_L^2}{2p^2 + i\omega\tau_e Z_L^2}\right):$$
$$\text{Rouse of linear at high } \omega \quad (A18b)$$

$$+ G_N(1 + \alpha)\phi_a\int_0^1(1 - VF_a s_a)^\alpha\frac{i\omega\tau_{a,b}(s_a)}{1 + i\omega\tau_{a,b}(s_a)}ds_a:$$
$$\text{Arm retraction} \quad (A18c)$$

$$+ G_N(1 + \alpha)\phi_l\int_0^{s_{TD}}(1 - VF_l s_l)^\alpha\frac{i\omega\tau_{l,b}(s_l)}{1 + i\omega\tau_{l,b}(s_l)}ds_l:$$
$$\text{Long linear in CLF} \quad (A18d)$$

$$+ G_N\phi_l(1 - s_{TD})\int_{\tau_a}^{\tau_C}\frac{\Phi(\tau)^\alpha}{2\tau}\frac{i\omega\tau}{1 + i\omega\tau}d\tau:$$
$$\text{CR motion of remaining long linear} \quad (A18e)$$

$$+ G_N(1 + \alpha)\phi_l^{\alpha+1}\int_{s_{TD}}^{s_{f,TD}}(1 - s_f)^\alpha\frac{i\omega\tau_{l,TD}(s_f)}{1 + i\omega\tau_{l,TD}(s_f)}ds_f:$$
$$\text{Long linear in CLF after } \tau_C \quad (A18f)$$

$$+ G_N[\phi_l(1 - s_{f,TD})]^{\alpha+1}\sum_{k=odd}\frac{8}{\pi^2 k^2}\frac{i\omega\tau_{d,TD}}{k^2 + i\omega\tau_{d,TD}}:$$
$$\text{Reptation of linear in the diluted tube} \quad (A18g)$$

A2. Reptation in an Undilated Tube. UDT. In UDT mode, the CR tube Rouse motion is assumed not to occur so reptation of long linear polymers proceeds unhindered in the undilated (original) tube. The reptation time $\tau_{d,UDT}$ is therefore determined as the crossover time between the time scales for CLF and the reptation in an undilated tube, (A9) and (A16*), respectively. Therefore, $\tau_{d,UDT}$ is $3\tau_e Z_L^3(1 - s_{f,UDT})^2$ with $s_{f,UDT}$ satisfying $3\tau_e Z_L^3(1 - s_l')^2 = \tau_{l,b}(s_l')$. The full expression for $G(\omega)$ of the UDT mode is obtained by removing the contributions of (A18e) and (A18f) and replacing (A18d) and (A18g) with the following contributions:

$$G_N(1 + \alpha)\phi_l\int_0^{s_{f,UDT}}(1 - VF_l s_l)^\alpha\frac{i\omega\tau_{l,b}(s_l)}{1 + i\omega\tau_{l,b}(s_l)}ds_l:$$
$$\text{CLF of long linear} \quad (A18d\text{ UDT})$$

$$G_N[\phi_l(1 - s_{f,UDT})]^{\alpha+1}\sum_{k=odd}\frac{8}{\pi^2 k^2}\frac{i\omega\tau_{d,UDT}}{k^2 + i\omega\tau_{d,UDT}}:$$
$$\text{Reptation in the original tube} \quad (A18g\text{ UDT})$$

A3. Reptation in Undilated Tube after CR Motion. UDT with CR. In UDT wCR mode, the CR tube Rouse motion is assumed to occur but reptation of long linear polymers in the undilated tube governs terminal relaxation. The reptation time in the undilated tube, $\tau_{d,UDTCR}$, is determined at the crossover time between the time scales for CLF in the dilated tube and the reptation in the original tube, (A17) and (A16*), respectively. Therefore, the reptation time, $\tau_{d,UDTCR}$ is $3\tau_e Z_L{}^3 (1 - s_{f,UDTCR})^2$ with $s_{f,UDTCR}$ satisfying $3\tau_e Z_L{}^3(1 - s_l')^2 = \tau_{l,TD}(s_l')$. The full expression for $G(\omega)$ of UDT with CR mode can be obtained by replacing (A18f) and (A18g) with the following contributions:

$$G_N(1 + \alpha)\phi_l{}^{\alpha+1} \int_{s_{TD}}^{s_{f,UDTCR}} (1 - s_f)^\alpha \frac{i\omega\tau_{l,TD}(s_f)}{1 + i\omega\tau_{l,TD}(s_f)} ds_f:$$
$$\text{CLF of long linear after } \tau_C$$

$$G_N[\phi_l(1 - s_{f,UDTCR})]^{\alpha+1} \sum_{k=odd} \frac{8}{\pi^2 k^2} \frac{i\omega\tau_{d,UDTCR}}{k^2 + i\omega\tau_{d,UDTCR}}:$$
$$\text{Reptation in the original tube}$$

B. Short Linear/Long Linear Blends. The effective fraction of unrelaxed segments $\Phi(s_i)$ and the effective potential $U_{i,b}(s_i)$ for short linear/long linear blends are defined as follows:

$$\Phi(s_l) = 1 - \underline{VF_l}\, s_l = 1 - \left(\phi_l + \phi_s\sqrt{\frac{Z_L}{Z_S}}\right)s_l \quad \text{(B1)}$$

$$\Phi(s_s) = 1 - \underline{VF_s}\, s_s = 1 - \left(\phi_s + \phi_l\sqrt{\frac{Z_S}{Z_L}}\right)s_s \quad \text{(B2)}$$

$$U_{i,b}(s_i) = \frac{3Z_i}{2} \frac{1 - (1 - VF_i s_i)^{\alpha+1}[1 + (1 + \alpha)VF_i s_i]}{VF_i{}^2(1 + \alpha)(2 + \alpha)} \quad \text{(B3)}$$

Here, the fraction of unrelaxed segments $\Phi(s_i)$ is expressed in terms of the fractional distance s_i with the factor VF_i derived from the Ball–McLeish equation.[6,7,21] The subscript i indicates s (or S) and l (or L), short linear and long linear chains, respectively.

The *early fast diffusion* time of linear polymers is given by

$$\tau_{early}(s_i) = \frac{9\pi^3}{16}\tau_e\left[\frac{Z_i}{2}\right]^4 s_i{}^4 \quad \text{(B4)}$$

The *late diffusion* time of linear polymers is given by

$$\tau_{late}(s_i) = \sqrt{\frac{\pi^5}{6}}\tau_e\left[\frac{Z_i}{2}\right]^{3/2} \times$$
$$\frac{\exp[U_{i,b}(s_i)]}{\sqrt{s_i{}^2(1 - VF_i s_i)^{2\alpha} + \frac{1}{VF_i{}^2}\left(\frac{VF_i{}^2(1 + \alpha)}{3(Z_i/2)}\right)^{2\alpha/(1+\alpha)}\left(\Gamma\left[\frac{1}{1 + \alpha}\right]\right)^{-2}}} \quad \text{(B5)}$$

The combined retraction time $\tau_{i,b}(s_i)$ is defined as

$$\tau_{i,b}(s_i) = \frac{\tau_{early}(s_i)\exp[U_{i,b}(s_i)]}{1 + \exp[U_{i,b}(s_i)]\tau_{early}(s_i)/\tau_{late}(s_i)} \quad \text{(B6)}$$

The relaxation time of short linear polymers is determined as the crossover time between CLF and reptation in the original tube.[1] Thus, $\tau_{d,s} = 3\tau_e Z_S{}^3(1 - s_{f,s})^2$ with $s_{f,s}$ satisfying $\tau_{d,s}(s_s') = \tau_{s,b}(s_s')$, where $\tau_{d,s}(s_s') = 3\tau_e Z_S{}^3(1 - s_s')^2$.

B1. Reptation of Unrelaxed Sections of Long Linear Polymer in the Dilated Tube. TD. Following relaxation of short linear polymers, the fractional distance of long chains, s_{TD}, is determined by solving $\tau_{d,s} = \tau_{l,b}(s_l')$. At this time, the fraction of unrelaxed segments again reduces from $\Phi(\tau_{d,s}) = \Phi(s_{TD})$ to $\phi_l(1 - s_{TD})$. Thus, the same calculation methods in the section A1 provide the constraint release time $\tau_C = \tau_{d,s}(\Phi(s_{TD})/(\phi_l(1 - s_{TD})))^{2\alpha}$ with $\Phi(t)^{2\alpha} = \Phi(s_{TD})^\alpha\sqrt{\tau_{d,s}/t}$ and the reptation time in the dilated tube $\tau_{d,TD}$ is $\tau_{d,Sol}(s_{f,TD})$ with $s_{f,TD}$ satisfying $\tau_{d,Sol}(s_l') = \tau_{l,TD}(s_l')$ [using (A17) and (A16)].

The full expression for $G(\omega)$ with $G_e = (5/4)G_N$ is then[1,2,6,16]

$$G(\omega) =$$

$$G_e\phi_s\left(\frac{1}{5Z_S}\sum_{Sp=1}^{Z_S-1}\frac{i\omega\tau_e Z_S{}^2}{p^2 + i\omega\tau_e Z_S{}^2} + \frac{1}{Z_S}\sum_{Sp=Z_S}^{N_S}\frac{i\omega\tau_e Z_S{}^2}{2p^2 + i\omega\tau_e Z_S{}^2}\right):$$
$$\text{Rouse of short at high } \omega \quad \text{(B7a)}$$

$$+ G_e\phi_l\left(\frac{1}{5Z_L}\sum_{Lp=1}^{Z_L-1}\frac{i\omega\tau_e Z_L{}^2}{p^2 + i\omega\tau_e Z_L{}^2} + \frac{1}{Z_L}\sum_{Lp=Z_L}^{N_L}\frac{i\omega\tau_e Z_L{}^2}{2p^2 + i\omega\tau_e Z_L{}^2}\right):$$
$$\text{Rouse of long at high } \omega \quad \text{(B7b)}$$

$$+ G_N(1 + \alpha)\phi_s\int_0^{s_{f,s}}(1 - VF_s s_s)^\alpha\frac{i\omega\tau_{s,b}(s_s)}{1 + i\omega\tau_{s,b}(s_s)}ds_s:$$
$$\text{Short linear in CLF} \quad \text{(B7c)}$$

$$+ G_N[1 - VF_s s_{f,s}]^\alpha[\phi_s(1 - s_{f,s})]\sum_{k=odd}\frac{8}{\pi^2 k^2}\frac{i\omega\tau_{d,s}}{k^2 + i\omega\tau_{d,s}}:$$
$$\text{Reptation of short linear} \quad \text{(B7d)}$$

$$+ G_N(1 + \alpha)\phi_l\int_0^{s_{TD}}(1 - VF_l s_l)^\alpha\frac{i\omega\tau_{l,b}(s_l)}{1 + i\omega\tau_{l,b}(s_l)}ds_l:$$
$$\text{Long linear in CLF} \quad \text{(B7e)}$$

$$+ G_N\phi_l(1 - s_{TD})\int_{\tau_{d,s}}^{\tau_C}\frac{\Phi(\tau)^\alpha}{2\tau}\frac{i\omega\tau}{1 + i\omega\tau}d\tau:$$
$$\text{CR motion of remaining long linear} \quad \text{(B7f)}$$

$$+ G_N(1 + \alpha)\phi_l{}^{\alpha+1}\int_{s_{TD}}^{s_{f,TD}}(1 - s_f)^\alpha\frac{i\omega\tau_{l,TD}(s_f)}{1 + i\omega\tau_{l,TD}(s_f)}ds_f:$$
$$\text{Long linear in CLF after } \tau_C \quad \text{(B7g)}$$

$$+ G_N[\phi_l(1 - s_{f,TD})]^{\alpha+1}\sum_{k=odd}\frac{8}{\pi^2 k^2}\frac{i\omega\tau_{d,TD}}{k^2 + i\omega\tau_{d,TD}}:$$
$$\text{Reptation of linear in a dilated tube} \quad \text{(B7h)}$$

The underlined prefactor corresponds to an instantaneous drop in the modulus.[6,7,12]

B2. Reptation in Undilated Tube. UDT. As in Appendix A2, the reptation time of long linear chains in the undilated tube $\tau_{d,UDT}$ is determined as the crossover time between the time scales for CLF and reptation in the original tube, (B6) and (A16*), respectively. Therefore, $\tau_{d,UDT}$ is $3\tau_e Z_L{}^3(1 - s_{f,UDT})^2$ with $s_{f,UDT}$ satisfying $3\tau_e Z_L{}^3(1 - s_l') = \tau_{l,b}(s_l')$. The full expression

for $G(\omega)$ of UDT mode is obtained by removing the contributions of (B7f) and (B7g) and replacing (B7e) and (B7h) with the following contributions of long linear polymers.

$$G_N(1 + \alpha)\phi_l \int_0^{s_{f,UDT}}(1 - VF_l s_l)^\alpha \frac{i\omega\tau_{l,b}(s_l)}{1 + i\omega\tau_{l,b}(s_l)}ds_l:$$
$$\text{Long linear in CLF} \quad \text{(B7e UDT)}$$

$$G_N[\phi_l(1 - s_{f,UDT})]^{\alpha+1} \sum_{k=odd} \frac{8}{\pi^2 k^2} \frac{i\omega\tau_{d,UDT}}{k^2 + i\omega\tau_{d,UDT}}:$$
$$\text{Reptation in the original tube} \quad \text{(B7h UDT)}$$

B3. Reptation in Undilated Tube after the CR Motion. UDT with CR. As in A3, the reptation time of long linear chains in an undilated tube after τ_C, $\tau_{d,UDTCR}$, is determined as the crossover time between the time scales for CLF in a dilated tube and reptation in the original tube, (A17) and (A16*), respectively. Therefore, the reptation time is given by, $\tau_{d,UDTCR}$ is $3\tau_e Z_L^3(1 - s_{f,UDTCR})^2$ with $s_{f,UDTCR}$ satisfying $3\tau_e Z_L^3(1 - s_l')^2 = \tau_{l,TD}(s_l')$. $G(\omega)$ for UDT with CR can be obtained by replacing (B7g) and (B7h) with the following contributions:

$$G_N(1 + \alpha)\phi_l^{\alpha+1} \int_{s_{TD}}^{s_{f,UDTCR}}(1 - s_f)^\alpha \frac{i\omega\tau_{l,TD}(s_f)}{1 + i\omega\tau_{l,TD}(s_f)}ds_f:$$
$$\text{Long linear in CLF after } \tau_C$$

$$G_N[\phi_l(1 - s_{f,UDTCR})]^{\alpha+1} \sum_{k=odd} \frac{8}{\pi^2 k^2} \frac{i\omega\tau_{d,UDTCR}}{k^2 + i\omega\tau_{d,UDTCR}}:$$
$$\text{Reptation in the original tube}$$

The *late diffusion* times of linear polymer chains can be further reduced as follows, because the deep retraction approximation (when s is near unity) is more questionable for CLF motion of linear polymers[7]

$$\tau_{\text{late}}(s_l) \approx \sqrt{\frac{\pi^5}{6}}\tau_e\left[\frac{Z_L}{2}\right]^{3/2} \frac{\exp[U_{l,b}(s_l)]}{\sqrt{s_l^2(1 - VF_l s_l)^{2\alpha}}} \quad \text{(C1)}$$

$$\tau_{\text{late},Sol}(s_l) = \sqrt{\frac{\pi^5}{6}}\tau_{e,D}\left[\frac{Z_{LD}}{2}\right]^{3/2} \frac{\exp[U_{l,sol}(s_l)]}{\sqrt{s_l^2(1 - s_l)^{2\alpha}}} \quad \text{(C2)}$$

The difference between the calculated time scales using (A7), (B5) and (A14) and those using (C1) and (C2) was generally found to be negligible.

References and Notes

(1) Milner, S. T.; McLeish, T. C. B. *Phys. Rev. Lett.* **1998**, *81*, 725.
(2) Milner, S. T.; McLeish, T. C. B. *Macromolecules* **1997**, *30*, 2159.
(3) de Gennes, P. G. *J. Chem. Phys.* **1971**, *55*, 572.
(4) Doi, M.; Edward, S. F. *The Theory of Polymer Dynamics*; Oxford: Oxford, U.K., 1986.
(5) Marrucci, G. *J. Polym. Sci., Polym. Phys. Ed.* **1985**, *23*, 159.
(6) Milner, S. T.; McLeish, T. C. B.; Young, R. N.; Hakiki, A.; Johnson, J. M. *Macromolecules* **1998**, *31*, 9345.
(7) Lee, J. H.; Archer, L. A. *Macromolecules* **2002**, *35*, 6687.
(8) Doi, M.; Graessley, W. W.; Helfand, E.; Pearson, D. S. *Macromolecules* **1987**, *20*, 1900.
(9) Viovy, J. L.; Rubinstein, M.; Colby, R. H. *Macromolecules* **1991**, *24*, 3587.
(10) Struglinski, M. J.; Graessley, W. W. *Macromolecules* **1985**, *18*, 2630.
(11) Colby, R. H.; Rubinstein, M. *Macromolecules* **1990**, *23*, 2753.
(12) Park, S. J.; Larson, R.G. *Macromolecules* **2004**, *37*, 597.
(13) Watanabe, H.; Ishida, S.; Matsumiya, Y.; Inoue, T. *Macromolecules* **2004**, *37*, 1937.
(14) Tanaka, Y.; Takeuchi, Y.; Kobayashi, M.; Tadokoro, H. *J. Polym. Sci., Part A-2*, **1971**, *9*, 43.
(15) Rubinstein, M.; Colby, R. H. *J. Chem. Phys.* **1988**, *89*, 5291.
(16) Likhtman, A. E.; McLeish, T. C. B. *Macromolecules* **2002**, *35*, 6332.
(17) Fetters, L. J.; Lohse, D. J.; Richter, D.; Witten, T. A.; Zirkel, A. *Macromolecules* **1994**, *27*, 4639.
(18) Frischknecht, A. L.; Milner, S. T. *J. Rheol.* **2002**, *46*, 671.
(19) Pattamaprom, C.; Larson, R. G.; Van Dyke, T. J. *Rheol. Acta* **2000**, *39*, 517.
(20) Archer, L. A.; Juliani. *Macromolecules* **2004**, *37*, 1076.
(21) Frischknecht, A. L.; Milner, S. T.; Pryke, A.; Young, R. N.; Hawkins, R.; McLeish T. C. B. *Macromolecules* **2002**, *35*, 4801.
(22) McLeish, T. C. B.; et al. *Macromolecules* **1999**, *32*, 6734.

MA040080H